Lee, C. A., & Saier, M. H., Jr. (1983) *J. Biol. Chem. 258*, 10761-10767.
Lo, M. M. S., Barnard, E. A., & Dolly, J. O. (1982) *Biochemistry 21*, 2210-2217.
Lolkema, J. S., & Robillard, G. T. (1985) *Eur. J. Biochem. 147*, 69-75.
Lolkema, J. S., Ten Hoeve-Duurkens, R. H., & Robillard, G. T. (1985) *Eur. J. Biochem. 149*, 625-631.
Misset, O., Brouwer, M., & Robillard, G. T. (1980) *Biochemistry 19*, 883-890.
Ottolenghi, P., & Ellory, J. C. (1983) *J. Biol. Chem. 258*, 14895-14907.
Postma, P. W., & Lengeler, J. W. (1985) *Microbiol. Rev. 49*, 232-269.
Reider, E., Wagner, E. F., & Schweiger, M. (1979) *Proc. Natl. Acad. Sci. U.S.A. 76*, 5529-5533.
Robillard, G. T., & Blaauw, M. (1987) *Biochemistry 26*, 5796-5803.
Robillard, G. T., Dooijewaard, G., & Lolkema, J. (1979) *Biochemistry 18*, 2984-2989.
Roossien, F. F., & Robillard, G. T. (1984) *Biochemistry 23*, 5682-5685.
Roossien, F. F., Blaauw, M., & Robillard, G. T. (1984) *Biochemistry 23*, 4934-4939.
Roossien, F. F., van Es-Spiekman, W., & Robillard, G. T. (1986) *FEBS Lett. 196*, 284-290.
Saier, M. H., Jr. (1980) *J. Supramol. Struct. 14*, 281-294.
Saier, M. H., Jr., Feucht, B. U., & Mora, M. K. (1977) *J. Biol. Chem. 252*, 8899-8907.
Stephan, M., & Jacobson, G. R. (1986a) *Biochemistry 25*, 4046-4051.
Stephan, M., & Jacobson, G. R. (1986b) *Biochemistry 25*, 8230-8234.
Wray, W., Boulikas, T., Wray, V. P., & Hancock, R. (1981) *Anal. Biochem. 118*, 197-203.

Tyrosine and Carboxyl Protonation Changes in the Bacteriorhodopsin Photocycle. 1. M_{412} and L_{550} Intermediates†

Paul Roepe,‡,§ Patrick L. Ahl,‡,∥ S. K. Das Gupta,⊥ Judith Herzfeld,# and Kenneth J. Rothschild*,‡

Departments of Physics and Physiology and Program in Cellular Biophysics, Boston University, Boston, Massachusetts 02215, Francis Bitter National Magnet Laboratory, Massachusetts Institute of Technology, Cambridge, Massachusetts 02139, and Department of Chemistry, Brandeis University, Waltham, Massachusetts 02254

Received November 21, 1986; Revised Manuscript Received February 4, 1987

ABSTRACT: The role of tyrosines in the bacteriorhodopsin (bR) photocycle has been investigated by using Fourier transform infrared (FTIR) and UV difference spectroscopies. Tyrosine contributions to the $BR_{570} \rightarrow M_{412}$ FTIR difference spectra recorded at several temperatures and pH's were identified by isotopically labeling tyrosine residues in bacteriorhodopsin. The frequencies and deuterium/hydrogen exchange sensitivities of these peaks and of peaks in spectra of model compounds in several environments suggest that at least two different tyrosine groups participate in the bR photocycle during the formation of M_{412}. One group undergoes a tyrosinate → tyrosine conversion during the $BR_{570} \rightarrow K_{630}$ transition. A second tyrosine group deprotonates between L_{550} and M_{412}. Low-temperature UV difference spectra in the 220-350-nm region of both purple membrane suspensions and rehydrated films support these conclusions. The UV spectra also indicate perturbation(s) of one or more tryptophan group(s). Several carboxyl groups appear to undergo a series of protonation changes between BR_{570} and M_{412}, as indicated by infrared absorption changes in the 1770-1720-cm^{-1} region. These results are consistent with the existence of a proton wire in bacteriorhodopsin that involves both tyrosine and carboxyl groups.

Bacteriorhodopsin (bR),[1] the M_r 26 000 integral protein in the purple membrane of *Halobacteria halobium*, functions as a light-driven proton pump (Stoeckenius & Bogomolni, 1982). During this photochemical process, the protein proceeds through a series of intermediates characterized by their visible absorption maxima. Recent evidence indicates that formation of the early photointermediate K involves several molecular events including (i) the isomerization of the all-trans chromophore about the 13-14 double bond (Braiman & Mathies, 1982), (ii) a substantial alteration in the local environment of the protonated Schiff base which is consistent with predicted charge separation from a counterion (Honig et al., 1979; Rothschild et al., 1984), and (iii) the protonation of a tyrosinate ion along with the perturbation of a tryptophan residue (or residues) (Rothschild et al., 1986). Further steps in the

† Supported by grants from the NIH and NSF to K.J.R. and from the NIH to J.H.
* Correspondence should be addressed to this author at the Department of Physics, Boston University.
‡ Boston University.
§ Present address: Department of Biochemistry, Roche Institute of Molecular Biology, Nutley, NJ 07110.
∥ Present address: Bio/molecular Engineering Branch, Naval Research Laboratory, Washington, DC 20375.
⊥ Massachusetts Institute of Technology.
Brandeis University.

[1] Abbreviations: $^2H/H$, deuterium/hydrogen; PM, purple membrane; bR, bacteriorhodopsin; [$^2H_4$]Tyr, ring-perdeuteriated L-tyrosine; bR-[$^2H_4$]Tyr, [$^2H_4$]Tyr-incorporated bacteriorhodopsin; FTIR, Fourier transform infrared.

0006-2960/87/0426-6696$01.50/0

bR photocycle need to be examined in order to deduce how these events and others are coupled to proton translocation and energy transduction.

In this paper, we report on results of FTIR and UV difference measurements that probe changes occurring by the M_{412} stage of the bR photocycle. It is known that M_{412} formation is accompanied by deprotonation of the retinylidene Schiff base (Lewis et al., 1974) and protonation of a carboxylate ion (or ions) (Rothschild et al., 1981; Siebert et al., 1982; Bagley et al., 1982). More recently, it has been shown that formation of the carboxyl group(s) which gives (give) rise to a 1761-cm^{-1} vibration is due to an Asp residue (or residues) (Engelhard et al., 1985). A second carboxyl group may also protonate, producing a smaller 1739-cm^{-1} peak (Engelhard et al., 1985). The formation of a tyrosinate ion and perturbation of a tryptophan residue at this stage of the photocycle have also been predicted on the basis of UV absorption changes above 280 nm (Bogomolni et al., 1978; Czege et al., 1982; Hess & Kushmitz, 1979; Bogomolni et al., 1980; Kushmitz & Hess, 1982; Sabés et al., 1984).

We now are able to demonstrate that a tyrosinate group is formed between L_{550} and M_{412} and that this group may be distinct from a tyrosinate present in BR_{570} which protonates by K_{630}. We also find evidence for the participation of several carboxyl groups and one or more tryptophan residues in the $BR_{570} \rightarrow M_{412}$ transition. These findings are consistent with movement of one or more hydrogen ions within a proton transport chain involving the protonations/deprotonations of tyrosines and carboxyls and hydrogen bond perturbations of tryptophan.

Materials and Methods

Materials. [$^2H_4$]Tyr was prepared by first converting L-[*ring*-$^2H_5$]Phe (Mathews et al., 1977) to *p*-amino[$^2H_4$]Phe according to procedures to be described elsewhere (Rice et al., unpublished results), diazotizing, and then hydrolyzing by refluxing in water. The product was isolated and purified by passage over AG50W-X8 cationic exchange resin (Bio-Rad) in the hydrogen form. bR-[$^2H_4$]Tyr was prepared by growing *H. halobium* R1 in a synthetic medium like that of Gochnauer and Kushner (1969), except that the D-amino acids and the NH_4Cl were omitted and that [$^2H_4$]Tyr with trace L-[*ring*-^3H]Tyr (New England Nuclear) was substituted for the unlabeled amino acid. PM sheets were isolated as described elsewhere (Oestehelt & Stoeckenius, 1973). Specific activity measurements indicated 50–80% of the tyrosine residues were labeled in various preparations. Amino acid analysis showed that less than 10% of the incorporated radioactivity scrambled to other amino acids, and ammonia–acetone extraction showed that less than 3% scrambled to lipids or retinal.

Films were made either from PM suspensions in distilled water by the isopotential spin dry method (Clark et al., 1980) or by slowly air-drying a concentrated drop of the PM suspension in buffer. In the later case, PM sheets were washed 3–5 times in 50 mM sodium phosphate buffer adjusted to a desired pH prior to film formation. Films were rehydrated with buffer by applying a drop directly over the dried film, equilibrating for 1–2 min, and then gently shaking off excess buffer. Water content of the film was monitored by comparing the integrated intensity of the water band at 3300 cm^{-1} to that of the amide I band. Ratios of approximately 6 to 1 or higher were considered indicative of adequate film hydration.

FTIR Spectroscopy. FTIR difference measurements were made on rehydrated PM films as described in detail elsewhere (Rothschild et al., 1984, 1985). "Photo-steady-state" $BR_{570} \rightarrow M_{412}$ difference spectra were computed by subtracting a BR_{570} spectrum recorded in the dark at or below 250 K from a spectrum recorded at the same temperature while illuminating the sample with yellow light (550-nm broad-band interference filter, Ditric Optics, Hudson, MA). This "off, yellow" illumination sequence was repeated up to 50 times, and the successive differences were averaged together. By examinination of successive 5-min dark scans obtained after illumination it was found at 250 K that thermal decay of M_{412} back to BR_{570} was complete within 5 min. "Thermal equilibrium" $BR_{570} \rightarrow M_{412}$ difference spectra at 220 K which contained decreased contributions from the L_{550} photoproduct compared to photo-steady-state spectra at this temperature, were also obtained. In this case, 15-min scans were recorded at 220 K and pH 7.0 by using the illumination sequence "off, yellow (550 nm), off, blue (450-nm broad-band filter, Ditric Optics)", and the two "off" scans were subtracted from each other in order to compute the difference spectrum. Again, up to 50 differences were averaged together. Contributions from the L_{550} intermediate in the photo-steady-state mixture decay out rapidly at this temperature and pH (Kalisky et al., 1981), whereas M_{412} exists in a stable form. Hence, the difference spectrum between the two "off" scans reflects mainly changes occuring between BR_{570} and M_{412}. It was found, by examining successive individual differences after the first illumination sequence, that photoreversal of the observed M_{412} with 450-nm light was complete under these conditions. A small percentage ($\approx$ 5–10%) of M produced in the first 550-nm flash is not photoconverted with 15 min of 450-nm illumination; however, this M is not in the presented spectra.

$BR_{570} \rightarrow L_{550}$ difference spectra were obtained with a slightly modified photo-steady-state method. For this experiment, a photo-steady-state difference was first obtained at 170 K. The film was then warmed to 220 K in the dark where the L_{550} intermediate was allowed to thermally decay for 15 min in the presence of 450-nm light (to photoconvert M_{412} produced by the L_{550} decay). The sample was then cooled back to 170 K and the process was repeated. Comparison of successive differences computed at 170 K revealed that all the L_{550} observed in the first difference cycled or decayed back to BR_{570} in 15 min at 220 K.

UV Difference Spectroscopy. UV difference measurements were made on humidified PM films deposited on Oriel quartz windows (Stanford, CT), and on PM suspensions in 70% glycerol. The films were produced by slow drying with a gentle stream of N_2 gas approximately 20 μL of a PM suspension at a protein concentration of approximately 2.5 mg/mL. This procedure produced a uniform film having an absorbance at 570 nm between 0.2 and 0.3 OD. The $BR_{570} \rightarrow M_{412}$ difference spectra of films were obtained at 220 K in a procedure similar to the thermal equilibrium FTIR experiments; i.e., both scans used to compute the difference spectrum were done in the dark before and after yellow illumination. Measurements were made using a Cary 219 UV/visible spectrophotometer equipped with a low-temperature cryostat (Janis, Waltham, MA) and a Scientific Instruments (West Palm Beach, FL) temperature controller. Light adaptation of the film prior to cooling to 220 K was accomplished with a 600-W tungsten lamp (Oriel, Stanford, CT) in combination with a Schott OG475 glass filter (Duryea, PA) and two heat filters (Edmund Scientific, Camden, NJ). Photoconversion to M_{412} at 220 K was performed with an Oriel 1000-W HgXe arc lamp in combination with an Oriel monochromator (Model 7240) and a narrow-band 570-nm interference filter (Ditric Optics). Photoreversal was accomplished at 220 K with 10 min of narrow-band 410-nm illumination by using the same light

source. By examination of spectra taken after several illumination sequences it was found both photoconversion and photoreversal were complete within 10 min of the respective illuminations. Spectra were recorded at 1-nm resolution.

Analysis of Data. FTIR difference spectra contain contributions from both chromophore and protein vibrational modes. Peaks due to tyrosine residues can be identified by comparing difference spectra of normal bR and bR containing isotopically labeled tyrosine. Since labeling induced alterations can be due to "normal" tyrosine peaks moving out of a spectral region, or "labeled" tyrosine modes moving into the region, we used both labeled and unlabeled tyrosine model compounds to distinguish between these two cases. In addition, because ionization of the tyrosine phenolic group alters the frequencies of some tyrosine modes, comparison with tyrosine model compounds at different pH's was necessary. A partial summary of the model compound data used in our analysis has been published elsewhere (Rothschild et al., 1986).

We also utilized a graphical method based on variable scaling to identify both the tyrosine and isotope-labeled tyrosine modes in the difference spectra. In theory, the subtraction between difference spectra of normal and tyrosine-labeled bR samples should result in a difference spectrum that contains peaks only due to tyrosine and labeled tyrosine modes. In practice, this requires scaling of the two spectra such that peaks originating from groups other than tyrosine cancel. However, perfect scaling can be difficult to achieve without an objective criteria for deciding which peaks do not contain tyrosine contributions. In order to circumvent this problem, we employ a range of scaling parameters. In this way, tyrosine and labeled tyrosine contributions can be independently identified.

This method is illustrated in the following example. Equations 1 and 2 represent spectral absorbance as a function of frequency for a normal $[f(\nu)]$ and tyrosine-labeled $[f'(\nu)]$ sample. The absorbance expressions contain two or three

$$f(\nu) = S(\nu) + T(\nu) \quad (1)$$

$$f'(\nu) = (1/\alpha)[S(\nu) + (q)T(\nu) + (1-q)T'(\nu)] \quad (2)$$

terms, respectively: eq 1 contains a term representing non-tyrosine contributions $[S(\nu)]$ and a second due to the tyrosine $[T(\nu)]$ contributions, whereas eq 2 contains an additional term $[T'(\nu)]$ representing labeled tyrosine contributions. The coefficient for $T(\nu)$ in eq 2, q, represents the small percentage of unlabeled tyrosine in the sample. The factor α in the eq 2 is introduced to account for differences in sample optical density which would multiply the absorbance equation by a constant factor.

As seen in eq 3, if these two spectra are subtracted by using a scaling factor (ϵ) for the labeled spectrum, the result contains three contributions. The first term represents either an ov-

$$\delta(\nu) = (1-\epsilon/\alpha)S(\nu) + (1-\epsilon q/\alpha)T(\nu) + [\epsilon(q-1)/\alpha]T'(\nu) \quad (3)$$

ershoot or undershoot in cancelation of the non-tyrosine contributions and will change sign when ϵ goes from less than α to greater than α. The second term is approximately independent of the scaling factor if q is small (i.e., if the percentage of labeled tyrosine is high). In this case, peaks due to tyrosine vibrational modes remain close to constant as the scaling factor is altered. Peaks due to the third term are directly proportional to the scaling factor and undergo a change in sign from the original $f'(\nu)$ spectrum. Hence, the contributions due to tyrosine should be identifiable in a set of curves represented by eq 3 with different ϵ factors *as those contributions that are approximately independent of* ϵ.

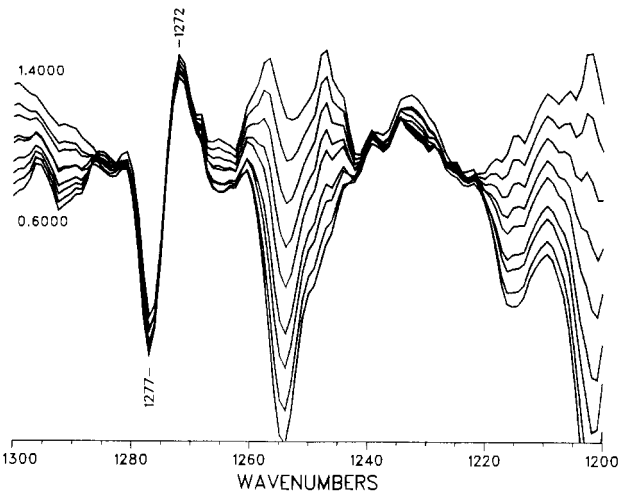

FIGURE 1: Example of variable subtraction factor method described under Analysis of Data. Nine plots are shown, each representing a normal bR difference spectrum at 220 K (see Figure 2 caption) minus a bR-[$^2H_4$]Tyr difference spectrum at 220 K that has been multiplied by a scaling factor, ϵ. Scaling factors ranged from 1.4 to 0.6 in steps of 0.1 for the subtractions presented. The largest non-tyrosine peaks were seen to change sign near $\epsilon = 0.86$. The deuteriated tyrosine sample was labeled at ≈80% efficiency as determined by specific activity measurements of tracer tritiated tyrosine (see Materials and Methods). Thus, with $q = 0.2$ and $\alpha = 0.85$, the largest possible variability in tyrosine peaks between the subtractions in this example should be ≈25%. The variability will be less for subtractions using ϵ factors close to α. The method has the added advantage of generating an unbiased scaling factor which can be used when comparing the two spectra visually. That is, the scaling factor which cancels contributions from peaks that do not contain tyrosine upon the subtraction can be used to mulitply or divide one of the spectra before visual comparison.

Figure 1 presents a set of curves produced by this method for the 1300–1200-cm^{-1} region. In this example, a bR-[$^2H_4$]Tyr spectrum recorded at 220 K (see Results) was subtracted from a normal bR spectrum recorded at the same temperature by using a range of scaling parameters. It is seen that the peaks at 1277 and 1272 cm^{-1} have appproximately constant intensity relative to the other peaks. The slight variation in integrated intensities (≈23%) is accounted for by incomplete labeling of the tyrosines in bR (see Figure 1 caption). An equivalent analysis can be performed to identify isotope-labeled tyrosine contributions by scaling eq 1 rather than eq 2 and then subtracting.

RESULTS

Evidence for a Tyrosinate Protonation by K_{630} That Persists through M_{412} Formation. The protonation of a tyrosinate group in BR_{570} during the formation of K_{630} was deduced in a recent low-temperature study of the $BR_{570} \rightarrow K_{630}$ transition (Rothschild et al., 1986). This conclusion was based on the close agreement between the characteristic frequencies of tyrosinate modes and negative (BR_{570}) tyrosine contributions in the spectrum and positive (K_{630}) contributions and the characteristic frequencies of tyrosine modes. Furthermore, only the positive peaks exhibited frequency shifts upon suspension of the sample in ^2H_2O. These shifts were very similar to those noted in model tyrosine compounds upon $^2H/H$ exchange of the phenolic hydrogen.

Figures 2 and 3 compare the difference spectra for bR and bR-[$^2H_4$]Tyr recorded at 220 K in H_2O under photo-steady-state conditions which as discussed below produce a mixture of L_{550} and M_{412}. Two sets of expanded spectra are shown in Figure 3 to demonstrate the reproducibility of the data. As indicated in Table I, *all of the positive tyrosine contributions*

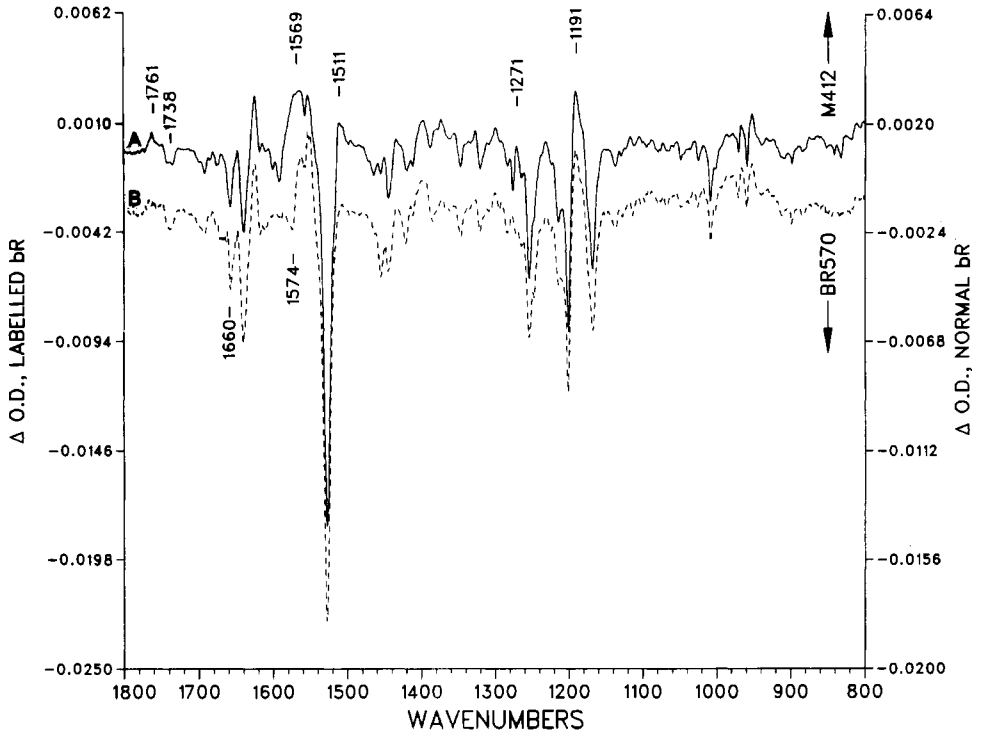

FIGURE 2: FTIR difference spectra obtained in a "photo-steady-state" experiment (see Materials and Methods) at 220 K, on PM films that were rehydrated with 50 mM phosphate buffer, pH 7.0. Solid line (A) is normal bR; dotted line (B) is bR-[$^2H_4$]Tyr. Spectra are scaled as under Analysis of Data ($\alpha = 0.85$) and by matching a majority of the peaks in the fingerprint region. This procedure results in excellent agreement with all peaks that do not contain tyrosine contributions. These include those at 1761, 1640, 1609, 1530, and 1167 cm^{-1}, as well as several others. The experiments were done with a Nicolet MX-1 spectrometer interfaced to a Nicolet 1200S data analysis and control system. Spectral resolution is 2 cm^{-1}. This resolution requires collection of 16K data points/scan. Each scan is 15 min long. A Happ–Genzel instrument line shape is applied to the interferogram before transformation. Each 15 min of scanning results in the acquistion of 480 interferograms. Mirror velocity on the MX-1 is fixed at 1.7 s/mirror travel path. FTIR spectrometer functions, illumination wavelength, and sample temperature were controlled using a forth program developed in our laboratory. Note the separate absorbance scale for each sample, due to differences in film thickness.

to the $BR_{570} \rightarrow K_{630}$ difference spectrum at 81 K are present at the higher temperature. For example, a positive 1511-cm^{-1} peak (cf. Figure 3A) is found which has previously been assigned to a tyrosine aromatic ring mode (Rothschild et al., 1986). In the $BR_{570} \rightarrow K_{630}$ difference spectrum this mode, which is found near 1514 cm^{-1}, is masked by the presence of the stronger 1515-cm^{-1} ethylenic stretch vibration of the K_{630} chromophore. At 220 K, where the concentration of K_{630} is much smaller, this peak is more apparent. In ^2H_2O it exhibits a slight downshift due to $^2H/H$ exchange of the tyrosine hydroxyl group (cf. Figure 5A) and becomes more intense possibly because less of the peak is canceled by the negative BR_{570} ethylenic stretch at 1530 cm^{-1}. Additional positive peaks assigned to a tyrosine group which are present in the difference spectra at both 81 and 220 K appear at 1456, 1240–1250,[2] 1210, and 828 cm^{-1} (cf. Figure 3 and Table I).

Almost all of the negative peaks assigned to a tyrosinate group at 81 K are observed at 220 K. For example, the 1276-cm^{-1} peak is at a characteristic frequency for the (predominantly) C–O$^-$ stretching vibration of the tyrosinate ion (Siamwiza, 1974) and is unaffected by the presence of ^2H_2O (cf. Figure 5B). Additional negative peaks at the two temperatures that are insensitive to $^2H/H$ exchange (cf. Figure 5A,C) are at 1411,[3] 842, and 833 cm^{-1}.

Identification of an Additional Set of Tyrosine and Tyrosinate Peaks at 220 K. In contrast to the $BR_{570} \rightarrow K_{630}$ difference spectrum at 81 K, an additional set of positive peaks that correlate well with *tyrosinate* vibrations were found at 220 K. We observe a small 1495-cm^{-1} peak (cf. Figure 3A) which is characteristic of a tyrosinate aromatic ring vibration. A second peak is found at 1271 cm^{-1} (cf. Figure 3B) which is in the range of the tyrosinate C–O$^-$ stretch. A third positive peak is found at 839 cm^{-1} (cf. Figure 3C) which may be due to the lower component of the Fermi doublet which shifts above 830 cm^{-1} when tyrosine is ionized (Siamwiza, 1974; Siamwiza et al., 1975; McHale, 1982). None of these peaks are affected by ^2H_2O, but all are shifted away due to the $^2H_4$ label. A negative shoulder at 1517 cm^{-1} which downshifts 2 cm^{-1} in ^2H_2O (cf. Figure 5A), characteristic of a tyrosine aromatic ring mode, is also identified. *These new peaks are consistent with the deprotonation of a tyrosine group that is originally present in BR_{570}.* Although one might intuitively expect positive and negative peaks representing the same vibrational modes to cancel each other partially or completely, it should be emphasized here that environmental effects on groups such as tyrosine can shift vibrational frequencies, thus

[2] The 1456 and 1240–1250-cm^{-1} peaks are believed to be masked positive peaks (Rothschild et al., 1986) superimposed on negative peaks at these frequencies. Since model compound data reveal that the tyrosine C–O phenoxyl stretch shifts down appproximately 25 cm^{-1} for both protonated and ionized forms, we attribute the effect between 1240 and 1250 cm^{-1} to the shifting down of tyrosinate C–O$^-$ stretches and the shifting out of tyrosine C–OH stretches. The tyrosinate stretch is slightly more intense than the tyrosine stretch in model compounds.

[3] The [$^2H_4$]Tyr-induced changes at 1411 cm^{-1} appear to be due to two effects. One is a shift from this frequency of a masked negative tyrosinate peak due to [$^2H_4$]Tyr labeling. The other is the appearance of a positive [$^2H_4$]tyrosine peak that shifts to near this frequency, presumably from 1456 cm^{-1}. Since the 1456-cm^{-1} peak is shifted upon phenoxyl $^2H/H$ exchange, we expect that the effect at 1411 cm^{-1} will be smaller for the bR spectra obtained in ^2H_2O. We do in fact find this to be the case (cf. Figures 3A and 5A).

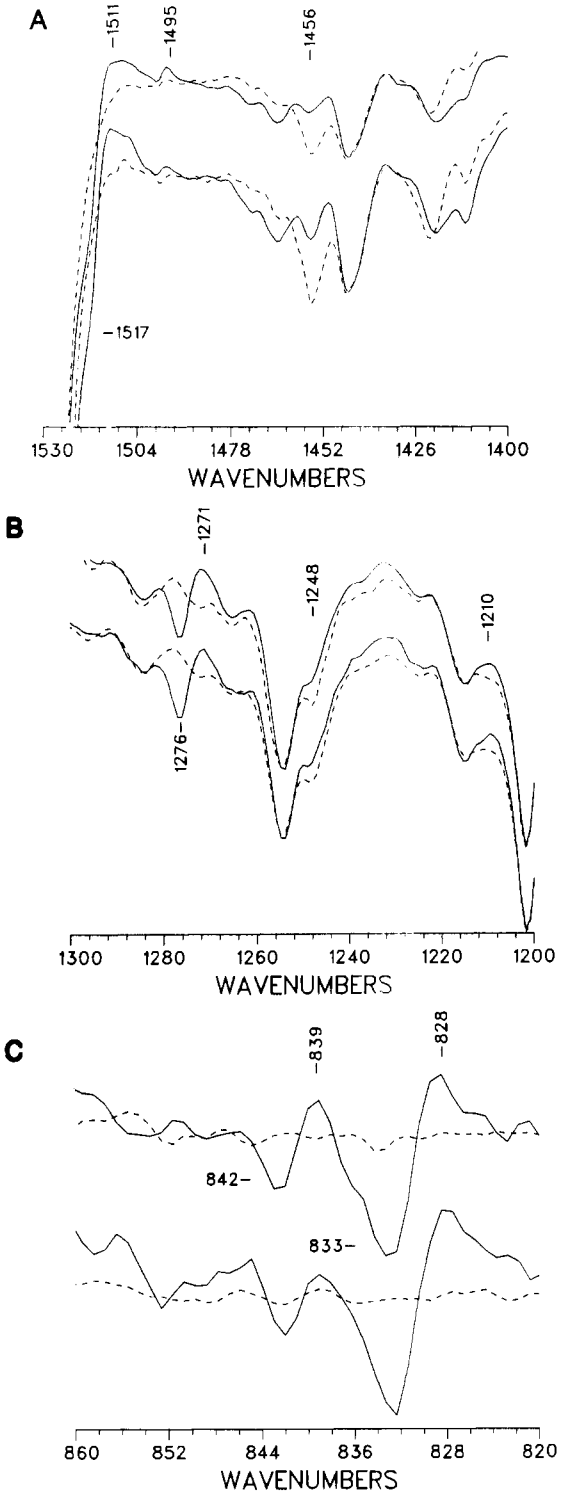

FIGURE 3: Same as in Figure 2, in expanded form. Four spectra are shown, each representing a different sample. Note in panel C that the increased noise is due simply to an expanded scale.

separating lines due to groups in different environments. This point is considered further under Discussion.

Evidence for a Tyrosine Deprotonation between L_{550} and M_{412}. The difference spectra shown in Figures 2–5 were recorded at 220 K under photo-steady-state conditions which promote the formation of both L_{550} and M_{412}. The presence of L_{550} in the photo-steady-mixture is evident from the appearance of characteristic positive chromophore peaks at 1540 and 1191 cm^{-1} (Argade & Rothschild, 1983) (cf. Figures 2 and 4). In order to eliminate contributions from L_{550}, we used three sets of conditions where M_{412} is dominant and L_{550} absent or greatly reduced. We also used a set of conditions to eliminate M_{412} and enrich for L_{550}. For example, a thermal equilibrium difference spectrum obtained at 220 K and pH 7.0 (see Materials and Methods) shows a marked reduction in the intensity of the L_{550} chromophore peaks (cf. Figure 6C), since L_{550} decays out of the photo-steady-state mixture during the second dark scan at this temperature (Kalisky et al., 1981). The positive 1562-cm^{-1} peak, due primarily to the chromophore ethylenic stretch of M_{412}, is now the most prominent positive peak in the spectrum. Other peaks near 1660 and 1650 cm^{-1} which may originate from amide I alterations are found to increase in intensity in the M_{412}-enriched spectrum.

The results of two additional M_{412}-enriching experiments are shown in parts A and B of Figure 6. These difference spectra were obtained under photo-steady-state conditions at 220 K and pH 9.5 and under photo-steady-state conditions at 250 K and pH 7.0, respectively. The elevated pH promotes

Table I: Tyrosine Peaks Identified in Difference Spectra[a]

BR → K, steady state, 81 K	BR → M, steady state, 220 K	BR → M, steady state, 250 K	assignments
1618 (+) BR	1618 (+) BR	1618 (+) BR	Tyr aromatic C=C stretch
1599 (+) BR, d	1599 (+) BR, d	1599 (+) BR, d	Tyr aromatic C=C stretch
1605–1585 (+) D	1605–1585 (+) D	1605–1585 (+) D	d-Tyr aromatic C=C stretch
1575 (–) D	1575 (–) D	1575 (–) D	d-tyrosinate
none	1517 (–) BR, d	1517 (–) BR, d	Tyr aromatic C=C stretch
1514 (+) BR, d	1511 (+) BR, d	1511 (+) BR, d	Tyr aromatic C=C stretch
1495–1465 (–) BR	1495 (+) BR	1495 (+) BR	tyrosinate C=C stretch
1456 (+) BR, d	1456 (+) BR, d	1456 (+) B, d	Tyr
1424 (–) D	1424 (–) D	1424 (–) D	d-tyrosinate
1419–1410 (+) D, d	1419–1410 (+) D, d	1419–1410 (+) D, d	d-Tyr
1411 (–) BR	1411 (–, +) BR	1411 (–, +) BR	tyrosinate
1277 (–) BR	1276 (–) BR	1277 (–) BR	tyrosinate C–O stretch
none	1273 (+) BR	1273 (+) BR	tyrosinate C–O stretch
1250–1240 (+) BR, d	1250–1240 (+, –) BR, d	1250–1240 (+, –) BR, d	Tyr C–O stretch
1248 (–) D	1248 (–, +) D	1248 (–, +) D	d-tyrosinate C–O stretch
none	1248–1240 (+) D	1248–1240 (+) D	d-tyrosinate C–O stretch
1210 (+) BR	1210 (+) BR	1210 (+) BR	Tyr
853 (–) BR	none	none	Tyr Fermi doublet
842 (–) BR	842 (–) BR	842 (–) BR	tyrosinate Fermi doublet
none	839 (+) BR	839 (+) BR	tyrosinate Fermi doublet
833 (–) BR	833 (–) BR	833 (–) BR	tyrosinate Fermi doublet
827 (+) BR, d	827 (+) BR, d	827 (+) BR, d	Tyr Fermi doublet

[a] Frequencies are given in cm^{-1}. Frequencies labeled with "BR" indicate peaks present in the normal ($BR_{570} \rightarrow K_{630}$ or $BR_{570} \rightarrow M_{412}$) difference spectra but not the isotope-labeled spectra. Those labeled with "D" indicate new peaks found in the isotope-labeled spectra. (+) or (–) indicates that peak is positive or negative, respectively. Note in some cases peaks in each direction are nearly degenerate and may cancel. "d" indicates the peak is $^2H/H$ exchange sensitive. Assignments were made on the basis of previous work (Siamwiza, 1974; Jakobsen & Brewer, 1962; Rothschild et al., 1986) as well as on the basis of model spectra including [$^2H_4$]Tyr and [$^2H_4$]tyrosinate.

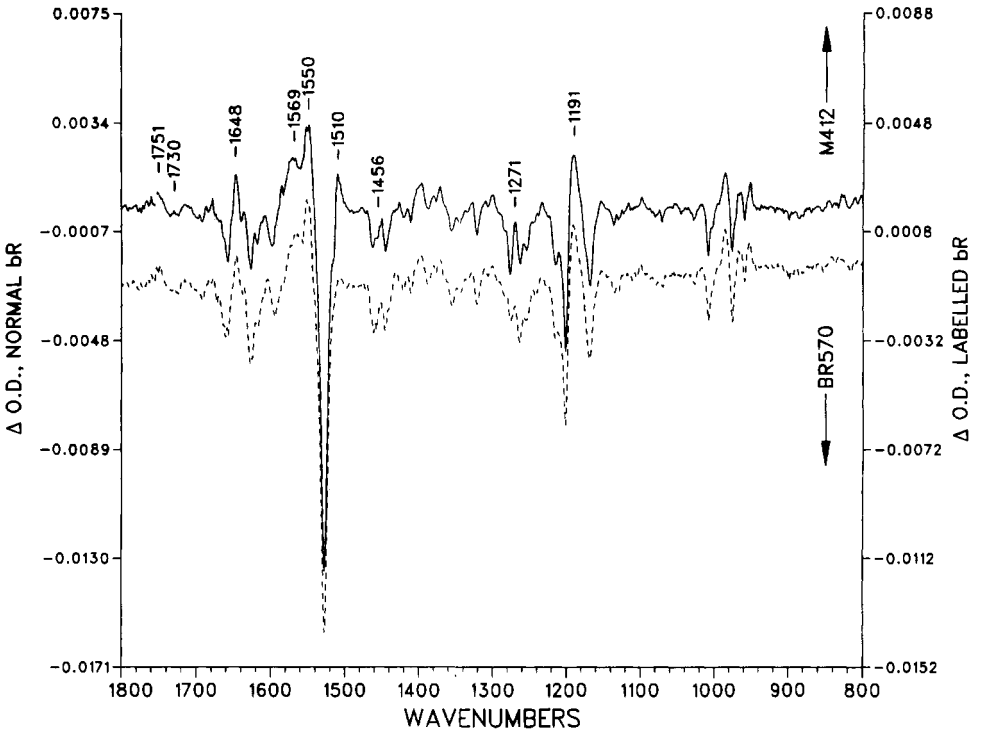

FIGURE 4: Same conditions as in Figure 2, except that the films were hydrated with unbuffered ^2H_2O.

the buildup of M_{412} as indicated by low-temperature visible absorption spectroscopy (Li et al., 1984). At the higher temperature L_{550} contributions are reduced because the intermediate is less stable. In both cases, we again find a reduction of characteristic L_{550} peaks and an increase in M_{412} peaks.[4]

Significantly, all of the difference spectra shown in Figure 6 that reflect enriched M_{412} and decreased L_{550} concentration display increased intensity of the positive 1495-, 1271-, and 839-cm^{-1} peaks, which have been assigned to tyrosinate vibrations. This can most clearly be seen in Figure 7, which superimposes the bR difference spectrum obtained at 220 K and pH 7.0 under photoequilibrium conditions with each of the four cases mentioned above.

We also utilized conditions that enhanced contributions from L_{550} and depleted contributions from M_{412} (cf. Figure 6D). It is seen the positive tyrosinate peaks at 1495, 1271, and 839 cm^{-1} are almost completely gone in this difference spectrum (cf. Figure 7A–C, bottom comparison). The negative 1517-cm^{-1} shoulder attributed to tyrosine is also not observed in this spectrum (data not shown). Interestingly, the 1660- and 1650-cm^{-1} peaks associated with amide I vibrations are nearly gone in this spectrum, indicating that the amide I alteration(s) occur between L_{550} and M_{412}.

Evidence for a Tyrosine Deprotonation between BR_{570} and M_{412} from UV Difference Spectra. Tyrosine protonation changes and hydrogen bond alterations can be monitored in the UV region of the spectrum (Donovan, 1969). Model compound studies have shown that tyrosine absorbance changes resulting from deprotonation are distinctly different from those arising due to hydrogen-bonding alterations (Strickland et al., 1972). Model compound studies in this laboratory (Rothschild et al., 1986) with poly(L-Tyr-Glu) show tyrosinate minus tyrosine difference spectra have relatively broad positive peaks at 243 ($\Delta\epsilon \approx 10\,000$ M^{-1} cm^{-1}) and 294 nm ($\Delta\epsilon \approx 2000$ M^{-1} cm^{-1}). In contrast, studies with tyrosine and *O*-methyltyrosine derivatives show that increased hydrogen bonding at the hydroxyl group produces only small (1–4-nm) red shifts in the absorption spectrum (Strickland et al., 1972). Our own results with cresol and *O*-methylcresol confirm this shift (unpublished data). This small absorbance shift results in the well-known double-peaked tyrosine perturbation spectrum with peaks near 280 and 285 nm (Donovan, 1969). Environmental perturbations of tryptophan by either electrostatic charge (Andrews & Forster, 1972) or hydrogen-bonding changes (Strickland et al., 1972) produce similarly shaped, but significantly red shifted, double-peaked features.

$BR_{570} \rightarrow M_{412}$ UV difference spectra obtained under three sets of conditions are shown in Figure 8. As seen in Figure 8B, the predominant photoproduct observed after illumination at 220 K is M_{412}. The long-wavelength region of each spectrum has an underlying negative slope to lower wavelengths due to the tail of M_{412} chromophore absorbance; however, each spectrum shows a broad absorbance increase in the 320–280-nm region centered near 300 nm that is consistent with a net tyrosine deprotonation. As would be expected for a UV deprotonation signal, there is also a larger peak (positive) at 238 nm in each spectrum. Several other common features are also observed. These include a large absorbance decrease at 272 nm and positive peaks at 288 and 297 nm. The features are more identifiable in the pH 10.9 spectrum due to the enhancement of M_{412} at high pH (see above). The most significant difference between the high-pH suspension and the film spectra are the relative heights of the 238- and 297-nm peaks, which could be due to orientation effects in the film.

The double-peaked features at 288 and 297 nm are assigned to the perturbation of one or more tryptophans, due to their significant red shift in relation to typical tyrosine perturbation peaks. The absorbance decrease at 270 nm is due in part to the tryptophan red shift(s), although some may be due to chromophore changes. Our observation of tryptophan alterations at this stage of the photocycle is in agreement with

[4] We also note several additional changes in chromophore and protein peaks due to the high-pH conditions are observed that cannot be attributed simply to an increase in M_{412} concentration. These include intensity increases near 1748, 1640, 1540, 1480, and 1260 cm^{-1} and intensity decreases near 1650, 1622, and 1194 cm^{-1} relative to major BR_{570} and M_{412} chromophore bands.

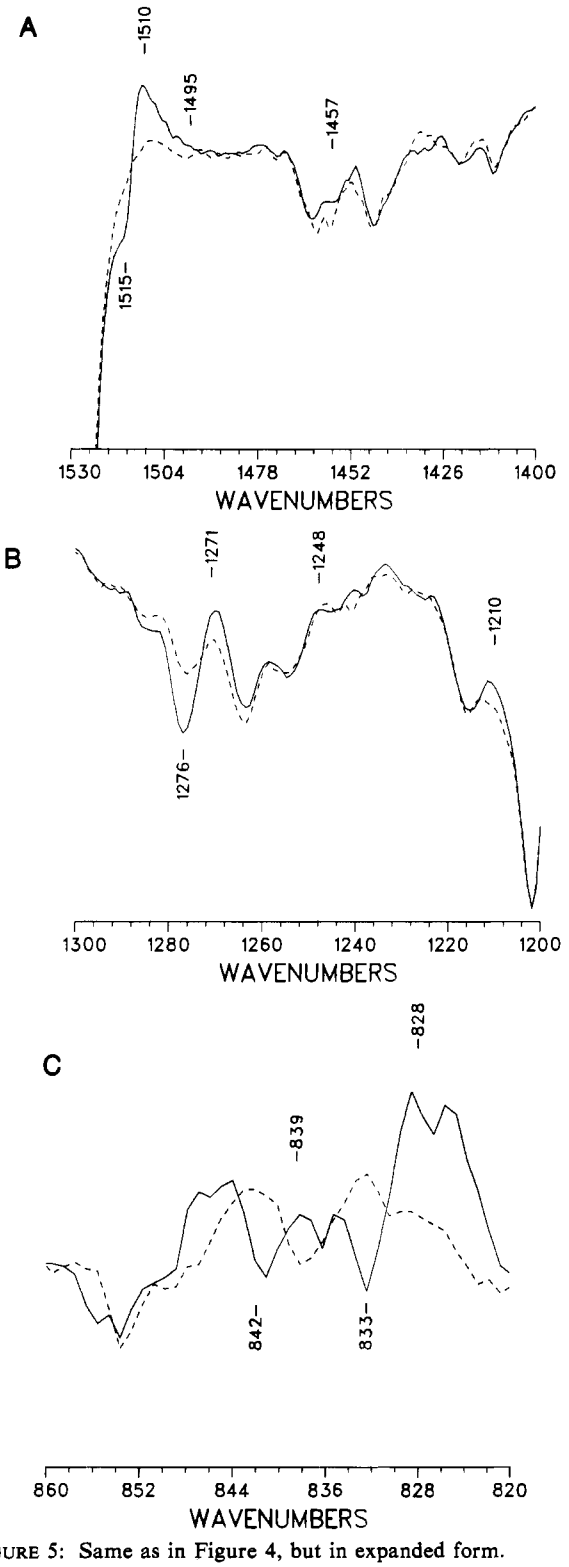

FIGURE 5: Same as in Figure 4, but in expanded form.

recent fourth derivative UV spectra of this photocycle transition (Sabes et al., 1984).

Figure 9A demonstrates that tyrosinate peaks observed in $BR_{570} \rightarrow M_{412}$ UV difference spectra at 220 K are not observed in the UV difference spectrum of a PM film obtained at 170 K in a manner similar to the FTIR $BR_{570} \rightarrow L_{550}$ spectrum (see above), or in an analogous difference spectrum obtained from a PM suspension. For both spectra in Figure 9A the clear positive M_{412} tyrosinate peaks at 240 and 300 nm are conspicuously absent. In contrast, a negative peak near 230–235 nm is visible, indicating that the tyrosinate protonation that is observed during K_{630} formation is not completely reversed by L_{550}, as also seen in the FTIR difference spectra. However, this peak is smaller than the negative peak at this wavelength in the $BR_{570} \rightarrow K_{630}$ UV difference spectrum (Rothschild et al., 1986). A positive peak at 294 nm is also discernible, possibly indicating a tryptophan hydrogen bond alteration. Figure 9B demonstrates that the L_{550} intermediate is preferentially observed in both experiments (see Figure 9 caption).

An estimate of the number of tyrosinates formed per M_{412} molecule can be obtained from the difference spectra by comparing the magnitude of the broad 280–320-nm positive tyrosinate peak to the magnitude of the negative chromophore peak at 578 nm. In order to avoid significant contributions from the 297-nm peak which has been assigned to a tryptophan perturbation, we used the absorbance increase at 302 nm for our estimate. A correct value of the absorbance change at 302 nm due solely to tyrosinate formation is difficult to obtain because of chromophore changes in this region. Model compound studies of Schiff base complexes (unpublished results) indicate the retinal chromophore contributions between 280 and 330 nm should be positive and essentially flat, with no major peaks or dips produced by Schiff base deprotonation and retinal $C_{13}{=}C_{14}$ double bond isomerization. Thus, we estimate the tyrosine absorbance contribution at 302 nm by extrapolating a constant positive chromophore absorbance "base line" from 330 nm. Using a 302-nm tyrosinate extinction coefficient change of 2000 M^{-1} cm and a 578-nm $BR_{570} \rightarrow M_{412}$ extinction coefficient change of 64 000 M^{-1} cm, we estimate the signal corresponds to net deprotonation of roughly 0.8–1.2 tyrosines per photocycling bR molecule. Although this is a rough estimate, it does indicate the magnitude of the positive peak we observe is compatible with single tyrosine protonation changes.

Carboxyl Group Involvement during the L_{550} to M_{412} Transition. Figure 10 compares the region from 1800–1700 cm^{-1} for the bR 220 K pH 7.0 photo-steady-state spectrum (Figure 2, top) with the M_{412}-enriched and L_{550}-enriched spectra (Figure 6). The 1761- and 1739-cm^{-1} positive peaks which have previously been associated with the protonation of carboxylate groups during M_{412} formation (Rothschild et al., 1981; Siebert et al., 1982; Bagley et al., 1982) are found to increase in the M_{412}-enriched spectra as expected. In the L_{550}-enriched spectrum a broad negative peak centered at the same frequency as the small positive 1739-cm^{-1} peak and a positive peak at 1748 cm^{-1} are observed. A small positive shoulder at 1755 cm^{-1} is also discernible. The broad negative peak has previously been associated with the deprotonation of a carboxyl during the $BR_{570} \rightarrow L_{550}$ transition (Engelhard et al., 1985).

Discussion

The primary conclusions that can be reached from this study are as follows: (i) A tyrosinate residue protonates by K_{630} and remains in the protonated state until M_{412}. (ii) A tyrosine residue deprotonates between L_{550} and M_{412}. (iii) Several carboxyl groups undergo protonation changes during the $L_{550} \rightarrow M_{412}$ transition. (iv) A tryptophan perturbation (or perturbations) occurs (occur) during formation of M_{412}.

The evidence for conclusions i and ii, which is in substantial agreement with Dollinger et al. (1986), is based on the appearance of positive tyrosinate peaks and a negative tyrosine peak in the $BR_{570} \rightarrow M_{412}$ but not the $BR_{570} \rightarrow L_{550}$ difference spectra. UV difference spectra exhibit positive tyrosinate peaks correlated with the formation of M_{412} but not L_{550}, strongly supporting these conclusions. There *also* exists a separate set of tyrosinate and tyrosine peaks indicative of a tyrosinate protonation which are already present at K_{630} and which persist

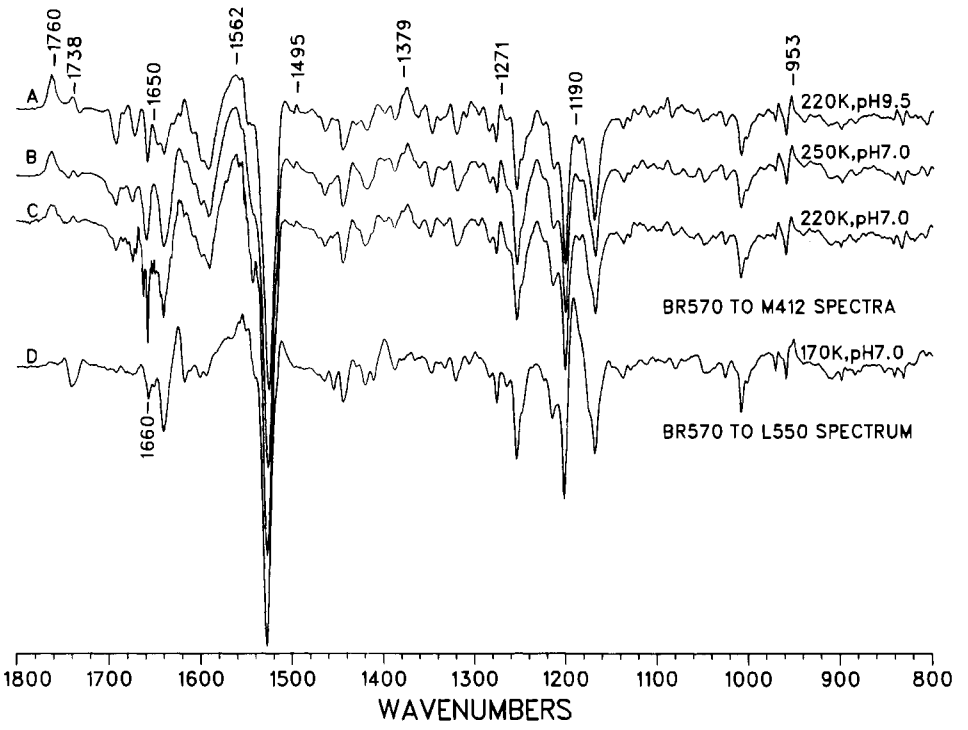

FIGURE 6: FTIR difference spectra at different temperatures and pH's: (A) photo-steady-state conditions (see Materials and Methods) at 220 K and pH 9.5; (B) photo-steady-state conditions at 250 K and pH 7.0; (C) thermal equilibrium conditions at 220 K and pH 7.0; (D) photo-steady-state conditions at 170 K and pH 7.0.

Chart I

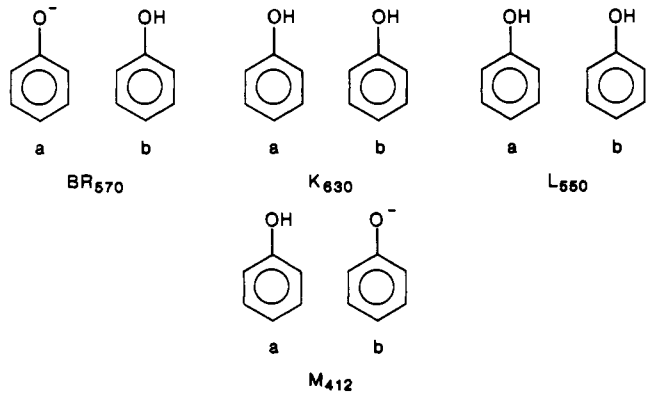

Chart II

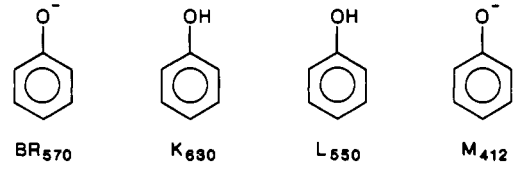

until M_{412}. These observations suggest changes of two separate tyrosines, one protonating by K_{630} and a second deprotonating by M_{412}, rather than the protonation of one group by K_{630} and its subsequent deprotonation by M_{412}. These alternate explanations are represented in Charts I and II, respectively.

Chart II as presented is not consistent with all of the FTIR data. For example, if one assumes that positive and negative tyrosinate peaks in the $BR_{570} \rightarrow M_{412}$ spectrum arise from a *single residue*, a change in environment near this residue could be invoked to explain the tyrosinate frequency shifts (e.g., from 1277 to 1271 cm^{-1}). However, Chart II would not account for negative tyrosine peaks in the $BR_{570} \rightarrow M_{412}$ difference spectrum which indicate a loss of tyrosine between BR_{570} and M_{412}. *In fact, a new negative peak at 1517 cm^{-1} assigned to a tyrosine group was found.*[5]

The UV spectra of the $B_{570} \rightarrow M_{412}$ and $BR_{570} \rightarrow L_{550}$ transitions also favor Chart I. As discussed, model compound studies show that positive peaks at 240 and 300 nm are characteristic of net tyrosine deprotonation but not changes in tyrosine or tyrosinate environment (Donovan, 1969; Strickland et al., 1972). Differences in extinction coefficient or extent of protonation of the two groups could produce net positive tyrosinate signals in the UV $BR_{570} \rightarrow M_{412}$ difference spectrum. Therefore, Chart II cannot easily explain the appearance of the positive 240- and 300-nm peaks in the $BR_{570} \rightarrow M_{412}$ UV difference spectrum.

Recent work has suggested that two forms of the M intermediate may be produced (Slifkin & Caplan, 1975; Lozier et al., 1976; Hess & Kushmitz, 1977; Ohno et al., 1981) upon excitation of BR_{570}. Furthermore, the relative percentages of these forms are affected by pH and temperature (Hanamoto et al., 1984; Li et al., 1984). It is possible that the presented $BR_{570} \rightarrow M_{412}$ difference spectra reflect the formation of both M forms, although temperatures below 278 K would be expected to enhance the observation of the slower decaying M form (Li et al., 1984). We cannot completely exclude the possibility, then, that the tyrosine deprotonation is specific to

[5] We were unable to identify additional negative tyrosine peaks in the M_{412}-enriched difference spectra; however, many of these peaks are expected to be nearly degenerate in frequency with positive peaks that arise from the protonation of a tyrosinate by K_{630}. Similarly, we would expect negative tyrosinate peaks which appear at the K_{630} stage to be partially or completely canceled by positive tyrosinate vibrations by M_{412}. In fact, we find a reduction in the intensity of several negative tyrosinate peaks (e.g., 1276 and 833 cm^{-1}) in comparing the M_{412}-enriched to the L_{550}-enriched difference spectra (cf. Figure 7). However, in this case *exact cancellation of tyrosinate* vibrations is less likely, since the frequencies of these modes are found to be more highly affected by environment than their *tyrosine* counterparts. For example, the C–O^- stretch frequency of tyrosinate has been observed to range between 1290 and 1260 cm^{-1} (Gaber et al., 1979; Que et al., 1980), while the tyrosine C–OH stretch remains within 5 cm^{-1} of 1245 cm^{-1} for a variety of model compounds under a variety of conditions (Rothschild et al., 1986).

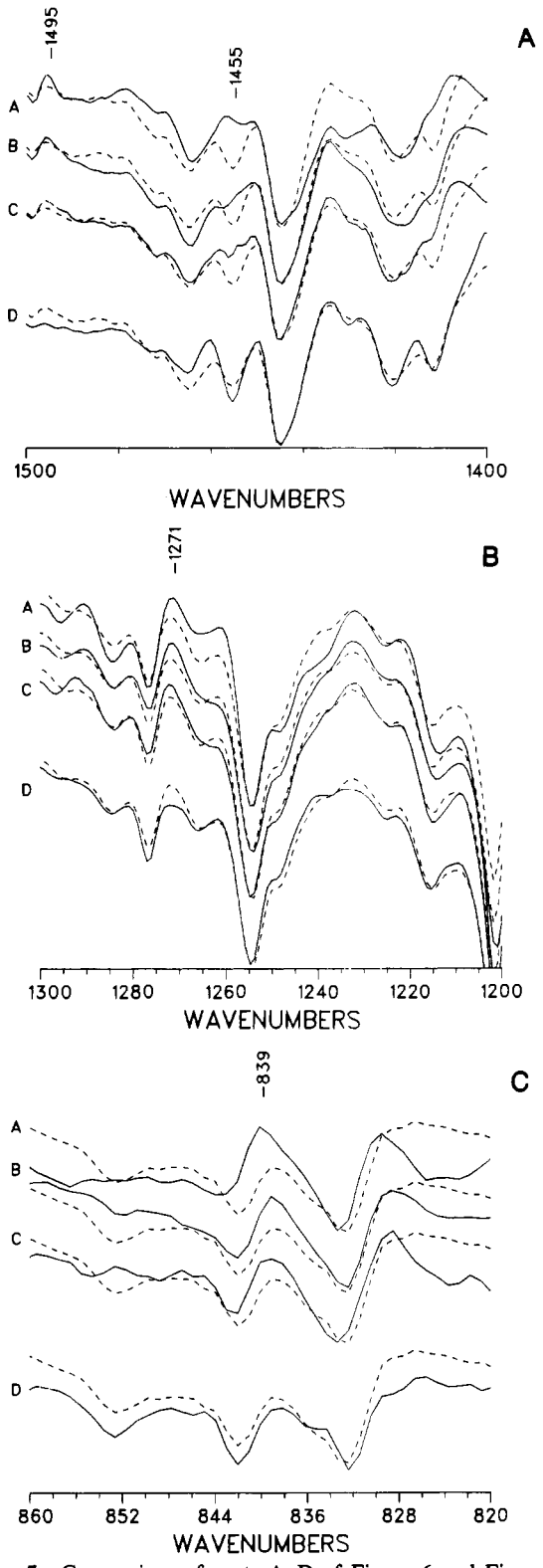

FIGURE 7: Comparison of parts A–D of Figure 6 and Figure 2A (dashed line) in several regions containing tyrosine contributions (see text).

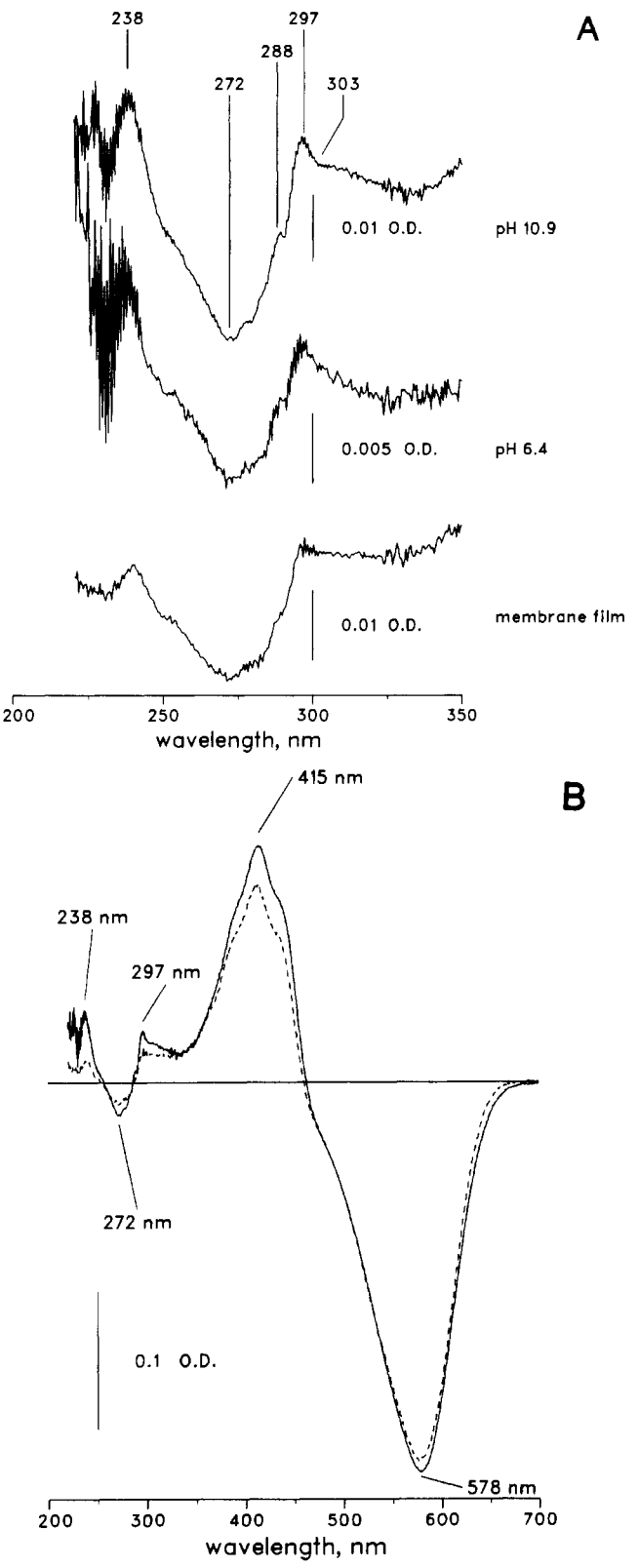

FIGURE 8: (A) UV difference spectra of the $BR_{570} \rightarrow M_{412}$ transition recorded at 220 K. (Top) PM suspended in 70% glycerol at pH 10.9; (middle) as in A but at pH 6.4; (bottom) spectrum obtained with a fully humidified PM film. Measurements were made at 1-nm resolution on a Cary 219 spectrophotometer interfaced to an Apple computer. (B) UV and visible regions of top (solid line) and bottom (dashed line) spectra of (A) to 700 nm. Spectra are not averaged and are unsmoothed. For experimental details, see Materials and Methods.

only one of the two M forms. However, we do observe (cf. Figures 6 and 7) that the intensities of the tyrosinate bands, relative to the intensities of chromophore bands, are very similar for the 250 K pH 7.0 and 220 K pH 9.5 photosteady-state experiments and the 220 K pH 7.0 thermal steady-state experiment. This indicates that, at these temperatures and pH's, if there is a change in the ratio of the two M forms, this change does not affect the tyrosine deprotonation signals. Further experiments currently under way using both low-temperature static and room temperature time-resolved FTIR difference spectroscopy (Braiman et al., 1985) under a variety of conditions may help to answer this question.

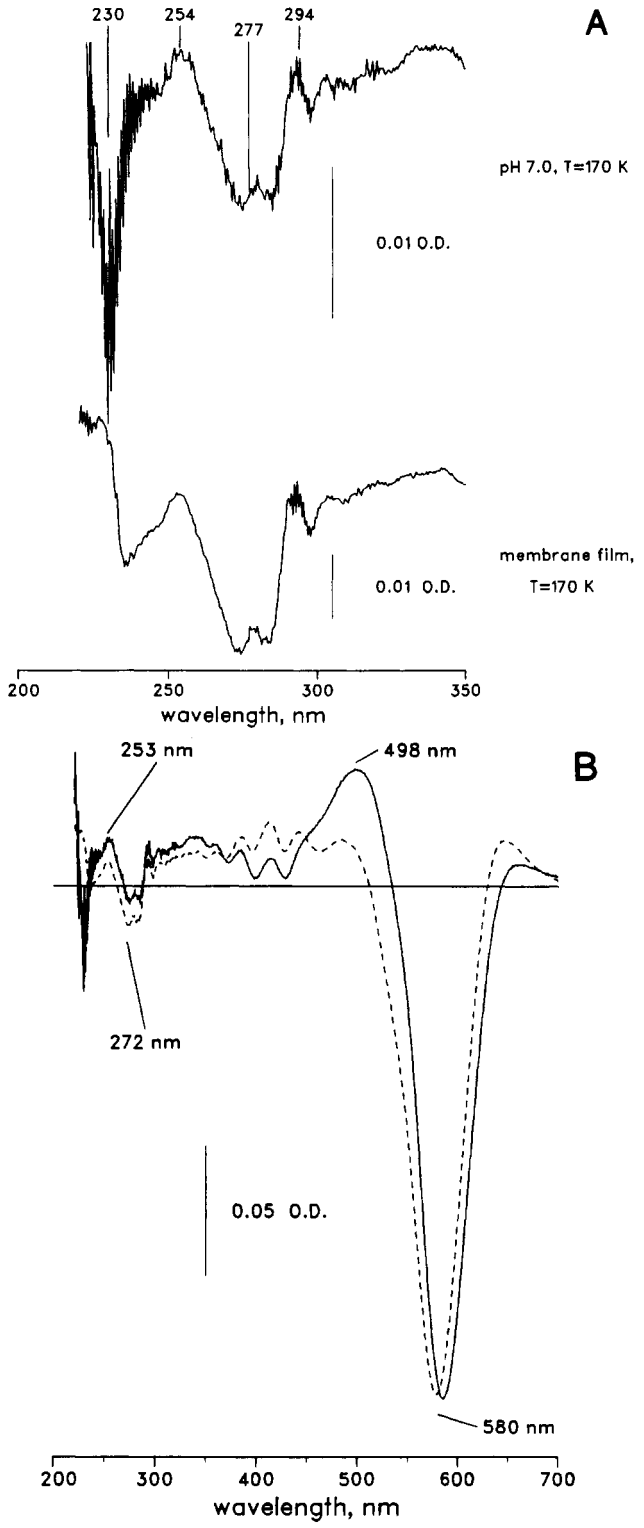

FIGURE 9: (A) UV difference spectra of the $BR_{570} \rightarrow L_{550}$ transition recorded at 170 K. (Top) PM suspension in 70% gycerol; (bottom) PM film, pH 7.0. Measurements were made as in Figure 8. (B) UV and visible regions of top (solid line) and bottom (dashed line) spectra of (A) to 700 nm. Note the peak at 498 nm due to the L_{550} chromophore absorbance. Although this peak is actually centered at 550 nm, much of it is canceled by the negative 570-nm peak due to the ground-state chromophore absorbance. No significant intensity near 412 nm is seen, indicating no appreciable M_{412} is produced under these conditions. Bars inserted indicate OD scale.

We note that there is some evidence that a third tyrosine group may be involved in the transition from BR_{570} to M_{412}. The FTIR evidence, presented in the following paper in this issue (Roepe et al., 1987), is derived mainly from studies with

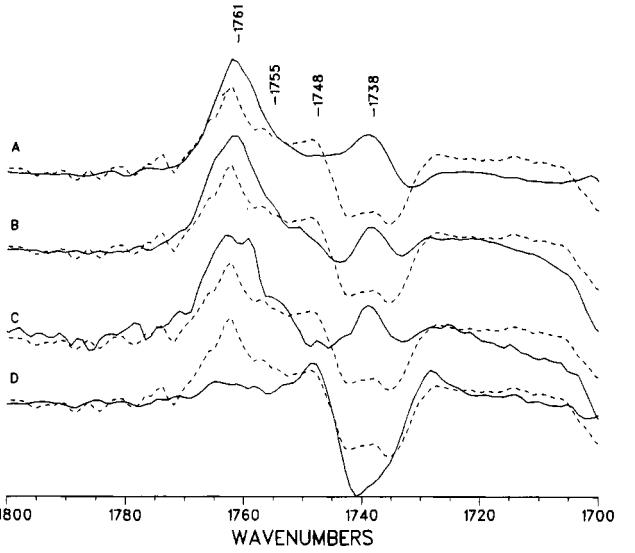

FIGURE 10: Comparison of parts A–D of Figure 6 and Figure 2A in the region 1800–1700 cm^{-1}. Dashed spectrum is Figure 2A, top solid line is Figure 6A, second solid line is Figure 6B, third solid line is Figure 6C, and bottom solid line is Figure 6D. Scale for Figure 6A is decreased slightly for comparison purposes.

Table II

no.	BR_{570}	K_{630}	L_{550}	M_{412}	frequency (cm^{-1})
1	COOH	COOH	COO^-	COOH	1739 (−)
2	COO^-	COO^-	COO^-	COOH	1739 (+)
3	COO^-	COO^-	COOH	COO^-	1748 (+)
4	COO^-	COO^-	COO^-	COOH	1760 (+)

selectively labeled Tyr-64, which appears to participate in the photocycle but which is not responsible for any of the tyrosinate peaks discussed above. The UV difference absorption data plus the FTIR data presented here and previously also suggest the possibility of a third tyrosine group which at least partially deprotonates between BR_{570} and L_{550}. That is, the large negative 240-nm peak in the $BR_{570} \rightarrow K_{630}$ UV difference spectrum is dramatically reduced in the $BR_{570} \rightarrow L_{550}$ difference spectrum[6] and then becomes positive in the $BR_{570} \rightarrow M_{412}$ difference spectrum. However, the 1277-cm^{-1} peak, as well as the other negative tyrosinate modes, does not decrease in intensity in the FTIR $BR_{570} \rightarrow L_{550}$ difference spectrum when compared to those in the $BR_{570} \rightarrow K_{630}$ difference spectrum. This could be explained if a third group, previously unidentified in the FTIR spectra, underwent at least partial deprotonation between K_{630} and L_{550}.

Conclusion iii is based on the observation of changes in the 1800–1700-cm^{-1} region characteristic of carboxyl group vibrations. While it is difficult at present to specify the exact number of carboxyl groups involved in the $BR_{570} \rightarrow L_{550}$ and $BR_{570} \rightarrow M_{412}$ transitions from the present data, our results are consistent with the following scheme: at least one carboxyl group deprotonates between K_{630} and L_{550} and then protonates before M_{412}, accounting for the growth and subsequent disappearance of the negative 1739-cm^{-1} peak. However, the size and asymmetrical shape of this peak in our spectrum (cf. Figure 10D) suggests more than one group may contribute.

[6] Although we cannot unequivocally state that the decrease in negative intensity at 240 and 300 nm in comparing $BR_{570} \rightarrow L_{550}$ to $BR_{570} \rightarrow K_{630}$ UV difference spectra is due to superimposed positive tyrosinate contributions that appear by L_{550}, chromophore differences at these wavelengths should be minimal when comparing the two spectra, since the K_{630} and L_{550} chromophores are both *cis*-$C_{13}{=}C_{14}$, *trans*-$C_{15}{=}N$ and protonated at the Schiff base.

A second carboxyl protonates between K_{630} and M_{412}, producing the narrower 1739-cm^{-1} band. There is also the possibility of a third group which protonates between K_{630} and L_{550}, giving rise to the positive flanking peak at 1748 cm^{-1}, which then must deprotonate at M_{412}, as the peak is lost in the enriched $BR_{570} \rightarrow M_{412}$ difference spectrum. At least one other carboxylate protonates between K_{630} and M_{412}, producing the 1761-cm^{-1} peak.[7] These changes are shown schematically in Table II.

It is interesting to note that there exist some similarities between the changes that occur in the carboxyl stretch region for bR and the related protein rhodopsin at the bathorhodopsin, lumirhodopsin, meta I, and meta II stages of bleaching (Rothschild et al., 1983; De Grip et al., 1985). In particular, a positive peak and a negative peak appear by the meta I intermediate at 1744 and 1726 cm^{-1}, respectively. These peaks, however, do not appear to be sensitive to $^2H/H$ exchange, contrary to those observed in the bR case (cf. Figure 4). Changes occur near 1740 and 1760 cm^{-1} in both the $L_{550} \rightarrow M_{412}$ transition and the meta I $\rightarrow$ meta II transition. Finally, recent studies (Rothschild et al., 1987; De Grip et al., 1985) show that the carboxyl alterations are reversed during meta II decay, similar to the reversal during the second half of the bR photocycle.

The observation of tryptophan hydrogen bond perturbations at this stage of the photocycle is in agreement with other UV spectroscopic studies (Hess & Kushmitz, 1979; Bogomolni et al., 1978; Sabês et al., 1984) of the $BR_{570} \rightarrow M_{412}$ transition. We cannot conclude whether the tryptophan perturbation that appears at K_{630} (Rothschild et al., 1986) is due to the same residue as that which is perturbed at M_{412}. We do notice rather large differences in the Trp perturbation peaks for the $BR_{570} \rightarrow K_{630}$ and $BR_{570} \rightarrow L_{550}$ difference spectra (including 3-nm shifts of the 297-nm M_{412} peak); thus, either the Trp perturbations observed at the three photocycle steps involve more than one group or environmental changes near a Trp group occur at L_{550}.

SUMMARY

In conclusion, the changes that occur in bacteriorhodopsin between the light-adapted BR_{570} and M_{412} intermediates appear to include the protonation of a tyrosinate, the deprotonation of at least one tyrosine, the perturbation of one or more tryptophans, and the changes in protonation of several carboxyl groups, as well as deprotonation of the Schiff base. These findings raise the possibility that we are observing spectroscopically the movement of one or more protons within some type of proton transport chain. In fact, proton wires of the type discussed by Nagle and Nagle (1983) as well as others (Eigen & DeMaeyer, 1958; Onsager, 1967, 1969; Nagle & Morowitz, 1978; Merz & Zundel, 1981; Tomchuk et al., 1985) can involve groups such as tyrosine, aspartate, and glutamate. Furthermore, these groups could exist in altered protonation states and may undergo concerted deprotonation/protonation reactions during proton transport involving the respective hydroxyl and carboxyl functionalities (Scheiner & Hillenbrand, 1985). Proximity of tryptophans to the tyrosines or carboxyls undergoing these reactions and/or helical structural changes that give rise to the peaks in the amide I region of the $BR_{570} \rightarrow M_{412}$ difference spectra could possibly account for the tryptophan spectral features we observe.

One model of a proton wire in bacteriorhodopsin envisions six hydrogen-bonded tyrosines in a "chain" between aspartate and glutamate hydrogen-bonded termini to the chain (Merz & Zundel, 1981). While tyrosine groups are not usually considered to be effective proton donors and acceptors under standard physiological conditions, it has been emphasized by Zundel that such a chain would still be capable of conducting charge via a Grotthus mechanism due to the polarizability of the hydrogen bonds. Similar considerations have been invoked to show how a tyrosine might act to protonate the Schiff base and perhaps serve as a counterion (Rastogi & Zundel, 1981; Christoforov et al., 1974). It should thus be possible for a tyrosine to act both as a counterion to the Schiff base and as a group involved in proton transport during the photocycle.

Although the proton wire interpretation of these tyrosine and carboxyl protonation changes is attractive on the basis of theoretical considerations, it should be emphasized that other explanations, including conformational changes that suddenly expose carboxyl groups to bulk water, could also be invoked to explain these protonation changes. Further progress will depend on a determination of the exact location in the amino acid sequence of the tyrosine and carboxyl groups observed to change protonation state during the bR photocycle. In this regard, we have examined in a related study the role of tyrosines-26 and -64 during the $BR_{570} \rightarrow K_{630}$ and $BR_{570} \rightarrow M_{412}$ steps of the photocycle by obtaining difference spectra of bR nitrated with high specificity at these tyrosines. The results from these studies are presented in the following paper (Roepe et al., 1987).

ACKNOWLEDGMENTS

We thank J. Gillespie, M. Tran, D. Gray, T. N. Earnest, and J. W. Courtemanche for expert technical assistance and Drs. S. Mohr, G. Jones, and M. S. Braiman for helpful discussions.

Registry No. L-Tyr, 60-18-4; L-Trp, 73-22-3.

REFERENCES

Andrews, L. J., & Forster, L. S. (1972) *Biochemistry 11*, 1875–1879.

Argade, P. V., & Rothschild, K. J. (1983) *Biochemistry 22*, 3460–3466.

Bagley, K., Dollinger, G., Eisenstein, L., Singh, A. K., & Zimanyi, L. (1982) *Proc. Natl. Acad. Sci. U.S.A. 79*, 4972–4976.

Bogomolni, R. A. (1980) in *Bioelectrochemistry* (Keysev, H., Ed.) pp 83–95, Plenum, New York.

Bogomolni, R. A., Stubbs, L., & Lanyi, J. (1978) *Biochemistry 17*, 1037–1041.

Braiman, M., & Mathies, R. (1982) *Proc. Natl. Acad. Sci. U.S.A. 79*, 403–407.

Braiman, M. S., Ahl, P. L., & Rothschild, K. J. (1985) in *Spectroscopy of Biological Molecules* (Alix, A. J., Bernard, L., & Manfait, M., Eds.) pp 57–59, Wiley-Interscience, New York.

Christoforov, V. L., Zvonkova, E. N., & Yevstigneyeva, R. P. (1974) *Zh. Obshch. Khim. 44*, 909–913.

Clark, N. A., Rothschild, K. J., Luippold, D., & Simons, B. (1980) *Biophys. J. 31*, 65–96.

Czege, J., Der, A., Zimanyi, L., & Keszthelyi, L. (1982) *Proc. Natl. Acad. Sci. U.S.A. 79*, 7273–7277.

De Grip, W., Gillespie, J., & Rothschild, K. J. (1985) *Biochim. Biophys. Acta 809*, 97–106.

Dollinger, G., Eisenstein, L., Lin, S.-L., Nakanishi, K., &

[7] An additional peak near 1755 cm^{-1} has also been postulated to appear by M_{412} (Engelhard et al., 1985) and appears as a shoulder in the 220 K photo-steady-state difference spectrum (cf. Figure 8). However, it is difficult for us to distinguish with the present data precisely at what photocycle step this peak appears.

Termini, J. (1986) *Biochemistry 25*, 6524–6533.
Donovan, J. W. (1969) in *Physical Principles and Techniques of Protein Chemistry* (Leach, S. J., Ed.) Part A, pp 101–170, Academic, New York.
Eigen, M., & DeMaeyer, L. (1958) *Proc. R. Soc. London, A 247*, 505–533.
Engelhard, M., Gerwert, K., Hess, B., Kreutz, W., & Siebert, F. (1985) *Biochemistry 24*, 400–407.
Gaber, B. P., Sheridan, J. P., Bazer, F. W., & Roberts, R. M. (1979) *J. Biol. Chem. 254*, 8340–8342.
Gochnauer, M. B., & Kushner, D. J. (1969) *Can. J. Microbiol. 15*, 1157–1165.
Hanamoto, J. H., Dupuis, P., & El-Sayed, M. A. (1984) *Proc. Natl. Acad. Sci. U.S.A. 81*, 7083–7087.
Hess, B., & Kushmitz, D. (1977) *FEBS Lett. 79*, 20–24.
Hess, B., & Kushmitz, D. (1979) *FEBS Lett. 100*, 334–340.
Honig, B., Ebrey, T., Callender, R. H., Dinur, U., & Ottolenghi, M. (1979) *Proc. Natl. Acad. Sci. U.S.A. 76*, 2503–2507.
Jakobsen, R. J., & Brewer, E. J. (1962) *Appl. Spectrosc. 16*, 32–35.
Kalisky, O., Ottolenghi, M., Honig, B., & Korenstein, R. (1981) *Biochemistry 20*, 649–655.
Kushmitz, D., & Hess, B. (1982) *FEBS Lett. 138*, 137–140.
Lewis, A., Spoonhower, J., Bogomolni, R. A., Lozier, R. H., & Stoeckenius, W. (1974) *Proc. Natl. Acad. Sci. U.S.A. 71*, 4462–4466.
Li, Q., Govindjee, R., & Ebrey, T. G. (1984) *Proc. Natl. Acad. Sci. U.S.A. 81*, 7079–7082.
Lozier, R. H., Niederberger, W., Bogomolni, R. A., Hwang, S. B., & Stoeckenius, W. (1976) *Biochim. Biophys. Acta 440*, 545–556.
Mathews, H. R., Mathews, K. S., & Opella, S. J. (1977) *Biochim. Biophys. Acta 497*, 1–13.
McHale, J. L. (1982) *J. Raman Spectrosc. 13*, 21–24.
Merz, H., & Zundel, G. (1981) *Biochem. Biophys. Res. Commun. 101*, 540–546.
Nagle, J. F., & Morowitz, H. J. (1978) *Proc. Natl. Acad. Sci. U.S.A. 75*, 298–302.
Nagle, J. F., & Nagle, S. T. (1983) *J. Membr. Biol. 74*, 1–14.
Oesterhelt, D., & Stoeckenius, W. (1973) *Methods Enzymol. 31*, 667–678.
Ohno, K., Takeuchi, Y., & Yoshida, M. (1981) *Photochem. Photobiol. 33*, 573–578.
Onsager, L. (1967) *Science (Washington, D.C.) 156*, 541.
Onsager, L. (1969) *Science (Washington, D.C.) 166*, 1359–1364.
Que, L., Heistand, R. H., Mayer, R., & Roe, A. L. (1980) *Biochemistry 19*, 2588–2593.
Rastogi, P. P., & Zundel, G. (1981) *Biochem. Biophys. Res. Commun. 99*, 804–812.
Roepe, P., Scherrer, P., Ahl, P. L., Das Gupta, S. K., Bogomolni, R. A., Herzfeld, J., & Rothschild, K. J. (1987) *Biochemistry* (following paper in this issue).
Rothschild, K. J., Zageski, M., & Cantore, B. (1981) *Biochem. Biophys. Res. Commun. 103*, 483–489.
Rothschild, K. J., Cantore, W., & Marrero, H. (1983) *Science (Washington, D.C.) 219*, 1333–1335.
Rothschild, K. J., Roepe, P., Lugtenburg, J., & Pardoen, J. A. (1984) *Biochemistry 23*, 6103–6109.
Rothschild, K. J., Roepe, P., & Gillespie, J. (1985) *Biochim. Biophys. Acta 808*, 140–148.
Rothschild, K. J., Roepe, P., Ahl, P., Earnest, T. N., Bogomolni, R. A., Das Gupta, S. K., Mulliken, C., & Herzfeld, J. (1986) *Proc. Natl. Acad. Sci. U.S.A. 83*, 347–351.
Rothschild, K. J., Gillespie, J., & DeGrip, W. J. (1987) *Biophys. J. 51*, 345–350.
Sabés, M., Duñach, M., Mañosa, J., Morros, A., & Padrós, E. (1984) *Photochem. Photobiophys. 8*, 97–101.
Scheiner, S., & Hillenbrand, E. A. (1985) *J. Phys. Chem. 89*, 3053–3060.
Siamwiza, M. N. (1974) Ph.D. Dissertation, Massachusetts Institute of Technology, Cambridge, MA.
Siamwiza, M. N., Lord, R. C., Chen, M. C., Takamatsu, T., Harada, I., Matsura, H., & Shimanouchi, T. (1975) *Biochemistry 14*, 4870–4876.
Siebert, F., Mäntele, W., & Kreutz, W. (1982) *FEBS Lett. 141*, 82–89.
Slifkin, M. A., & Caplan, S. R. (1975) *Nature (London) 253*, 56–58.
Stoeckenius, W., & Bogomolni, R. A. (1982) *Annu. Rev. Biochem. 52*, 587–616.
Strickland, E. H., Wilchek, M., Horowitz, J., & Billups, C. (1972) *J. Biol. Chem. 247*, 572–580.
Tomchuk, P. M., Procenko, N. A., & Krasnogolvets, U. V. (1985) *Biochim. Biophys. Acta 807*, 272–277.